Experimental demonstration of spectral broadening in an all-silica Bragg fiber

Henry T. Bookey,[1,*] Sonali Dasgupta,[2] Nagaraju Bezawada,[3] Bishnu P. Pal,[3] Alexey Sysoliatin,[4] John E. McCarthy[1], Mikhail Salganskii[5], Vladimir Khopin[5] and Ajoy K. Kar,[1]

[1]Nonlinear Optics Group, Department of Physics, School of Engineering and Physical Sciences, Heriot Watt University, Edinburgh, EH14 4AS, UK
[2]Optoelectronics Research Centre, University of Southampton, SO17 1BJ, UK,
[3]Physics Department, Indian Institute of Technology Delhi, 110016, India,
[4] FORC, Russian Academy of Sciences, Moscow, Russia,
[5]ICHPS Russian Academy of Sciences, Nizhny Novgorod, Russia
**h.t.bookey@hw.ac.uk*

Abstract: We present the first report on experimental observation of nonlinear spectral broadening in an all-solid photonic band gap Bragg fiber of relatively large mode area ~62 μm^2. The theoretically designed Bragg fiber for this specific application was fabricated by the well known MCVD technique. Nonlinear spectral broadening was observed by launching high power femtosecond pulses of 1067 nm pump wavelength. These first results indicate that fabrication of such Bragg fibers, once perfected, should potentially serve as an alternative route for realization of supercontinuum light.

OCIS codes: (060.4370) Nonlinear optics, fibers; (060.2280) Fibre design and fabrication; (060.2270) fiber characterization; (320.5550) Pulses.

References and links

1. Y. Fink, D. J. Ripin, S. Fan, C. Chen, J. D. Joannepoulos, and E. L. Thomas, "Guiding optical light in air using an all-dielectric structure," J. Lightwave Technol. **17**(11), 2039–2041 (1999).
2. P. Yeh, A. Yariv, and E. Marom, "Theory of Bragg fibers," J. Opt. Soc. Am. **68**(9), 1196–1201 (1978).
3. V. N. Melekhin, and A. B. Manenkov, "Dielectric tube as a low-loss waveguide," Zhurnal Technicheskoi Fiziki **38**, 2113–2115 (1968).
4. B. Temelkuran, S. D. Hart, G. Benoit, J. D. Joannopoulos, and Y. Fink, "Wavelength-scalable hollow optical fibres with large photonic bandgaps for CO2 laser transmission," Nature **420**(6916), 650–653 (2002).
5. G. Vienne, Y. Xu, C. Jakobsen, H. J. Deyerl, T. P. Hansen, B. H. Larsen, J. B. Jensen, T. Sorensen, M. Terrel, Y. Huang, R. Lee, N. A. Mortensen, J. Broeng, H. Simonsen, A. Bjarklev, and A. Yariv, "First demonstration of air-silica Bragg fiber," Optical Fiber Communication Conference (OFC) paper: PD25 (2004). URL *http://www.opticsinfobase.org/abstract.cfm?URI=URI=OFC-2004-P%*
6. E. Pone, C. Dubois, N. Gu, Y. Gao, A. Dupuis, F. Boismenu, S. Lacroix, and M. Skorobogatiy, "Drawing of the hollow all-polymer Bragg fibers," Opt. Express 14 (13), 5838–5852 (2006). URL *http://www.opticsexpress.org/abstract.cfm?URI=oe-14-13-5838*.
7. X. Feng, T. M. Monro, P. Petropoulos, V. Finazzi, and D. J. Richardson, "Extruded single-mode high-index-core one-dimensional microstructured optical fiber with high index-contrast for highly nonlinear optical devices," Appl. Phys. Lett. **87**(8), 081110 (2005).
8. F. Brechet, P. Roy, J. Marcou, and D. Pagnoux, "Single-mode propagation into depressed-core-index photonic bandgap fiber designed for zero-dispersion propagation at short wavelengths," Electron. Lett. **36**(6), 514–515 (2000).
9. S. Février, R. Jamier, J. M. Blondy, S. L. Semjonov, M. E. Likhachev, M. M. Bubnov, E. M. Dianov, V. F. Khopin, M. Y. Salganskii, and A. N. Guryanov, "Low-loss singlemode large mode area all-silica photonic bandgap fiber," Opt. Express **14** (2), 562–569 (2006). URL *http://www.opticsexpress.org/abstract.cfm?URI=oe-14-2-562*
10. J. R. Ott, M. Heuck, C. Agger, P. D. Rasmussen, and O. Bang, "Label-free and selective nonlinear fiber-optical biosensing," Opt. Express **16** (25), 20834–20847 (2008). URL *http://www.opticsexpress.org/abstract.cfm?URI=oe-16-25-20834*
11. J. Mandon, E. Sorokin, I. T. Sorokina, G. Guelachvili, and N. Picqu, "Supercontinua for high-resolution absorption multiplex infrared spectroscopy," Opt. Lett. **33** (3), 285–287 (2008).URL *http://ol.osa.org/abstract.cfm?URI=ol-33-3-285*.

#112382 - $15.00 USD Received 4 Jun 2009; revised 4 Sep 2009; accepted 5 Sep 2009; published 11 Sep 2009

12. B. P. Pal, S. Dasgupta, M. R. Shenoy, and A. Sysoliatin, "Supercontinuum generation in a Bragg fiber: A Novel Proposal," Optoelectron. Lett. **2**(5), 342–344 (2006).
13. S. Dasgupta, B. P. Pal, and M. R. Shenoy, "Nonlinear Spectral Broadening in Solid-Core Bragg Fibers," J. Lightwave Technol. **25**(9), 2475–2481 (2007).
14. S. Johnson, M. Ibanescu, M. Skorobogatiy, O. Weisberg, T. Engeness, M. Soljacic, S. Jacobs, J. Joannopoulos, and Y. Fink, "Low-loss asymptotically single-mode propagation in large-core OmniGuide fibers," Opt. Express **9**,748–779(2001) URL *http://www.opticsinfobase.org/abstract.cfm?URI=oe-9-13-748*
15. G. P. Agrawal, *Nonlinear Fiber Optics*, 2nd ed. (Academic Press, San Diego, 1995).
16. S. Février, R. Jamier, J.-M. Blondy, S. L. Semjonov, M. E. Likhachev, M. M. Bubnov, E. M. Dianov, V. F. Khopin, M. Y. Salganskii, and A. N. Guryanov, "Low-loss singlemode large mode area all-silica photonic bandgap fiber," Opt. Express **14** (2), 562–569 (2006). URL *http://www.opticsexpress.org/abstract.cfm?URI=oe-14-2-562*.
17. K. J. Rowland, S. A. V., and T. M. Monro, "Novel Low-Loss Bandgaps in all-silica Bragg Fibers," J. Lightwave Technol. **26** (1), 43–51 (2008). URL *http://jlt.osa.org/abstract.cfm?URI=JLT-26-1-43*
18. A. V. Husakou, and J. Herrmann, "Supercontinuum generation of higher-order solitons by fission in photonic crystal fibers," Phys. Rev. Lett. **87**(20), 203901 (2001).
19. P. Pal, and W. H. Knox, "End-sealing short dispersion micromanaged tapered holey fibers by hole-collapsing," Opt. Express **15**, 13531–13538 (2007). URL *http://www.opticsinfobase.org/abstract.cfm?URI=oe-15-21-13531vv*

1. Introduction

Bragg fibers are microstructured optical fibers, in which light is guided by the photonic band gap effect. The concentric cladding layers of alternate high and low refractive indices that symmetrically surround the low index central core of a Bragg fiber form a one dimensional radially periodic structure; the core could be of a lower or same refractive index as the lower of the two periodic layers that surround it. Radiation loss and dispersion of the propagating mode in them depend on size and refractive index of the core and refractive index contrast as well as thickness of the cladding layers. Thus, Bragg fibers offer a wide choice of parametric avenues to tailor their propagation characteristics. Incidentally, Bragg fibers were the very first variety of photonic band gap (PBG) fibers to be proposed (although the photonic band gap associated with them was not formally appreciated until 1999 [1]) in the literature and were theoretically studied as early as the late 1970s or even earlier [2,3]. However, limited fabrication technology stunted the development of these fibers until recently when the rapid progress in the field of microstructured fibers has revived interest in Bragg fibers. Besides silica, various unconventional material systems like chalcogenide glass, polymers and soft glass have been used to fabricate such fibers [4–7]. Whilst this renewed interest had focused largely on the design of air-core Bragg fibers, solid-core silica-based Bragg fibers have also attracted significant attention because of their ease in splicing to conventional fibers and their robustness to withstand structural degradation with time. Indeed, realization of solid core Bragg fiber with zero dispersion wavelength (ZDW) at 1060 nm has been the earliest milestone in this direction [8]. In addition to their widely tunable dispersion characteristics, solid core Bragg fibers can be designed to exhibit low loss, large mode effective area [9], and low or high sensitivity to nonlinear propagation effects. The possibility of exploiting nonlinear optical effects in these fibers along with zero dispersion wave-length around or below 1 μm wavelength whilst maintaining a large mode size is particularly appealing for potential applications in e.g. all-fiber pulse compression systems for Yb^{3+} doped fiber lasers, short pulse fiber delivery of femtosecond lasers, optical coherence tomography (OCT), optical bio-sensing [10], near-infrared spectroscopy [11], and so on. Photonic crystal fibers could also be designed to shift the ZDW to this wavelength region; however, typically, they would require a relatively smaller core size to maintain single-mode propagation. Consequently coupling of light to the fiber could be difficult at times and it could also limit the fiber's power handling capacity. In this paper we demonstrate nonlinear spectral broadening of femtosecond pulses of 1067 nm wavelength after propagation through a solid-core Bragg fiber, whose design was tailored for zero dispersion at around 1064 nm. The designed fiber parameters served as initial input to fiber fabricators for tuning the MCVD deposition process. We have also attempted a comparison of the estimated spectral broadening based on numerical simulation of nonlinear pulse propagation with one of the measured broadened spectra as a sample. The agreement was reasonable despite uncertainties in precise fiber parameters and conditions of the

#112382 - $15.00 USD Received 4 Jun 2009; revised 4 Sep 2009; accepted 5 Sep 2009; published 11 Sep 2009

experiment. To the best of our knowledge, this is the first experimental demonstration of nonlinear spectral broadening in a PBG Bragg fiber.

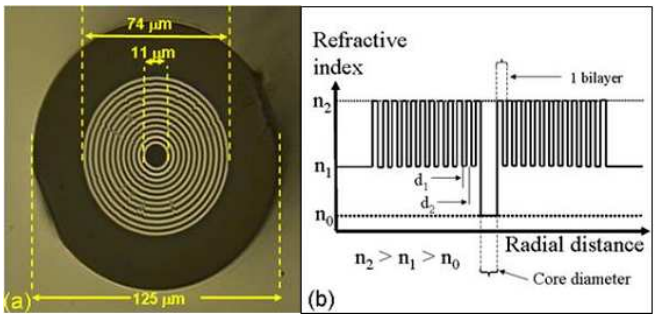

Fig. 1. (a) Optical microscope image of end facet of the fabricated Bragg fiber. (b) Schematic of index profile showing fiber geometry and nomenclature.

2. Fiber design, fabrication and measurements

The solid-core Bragg fiber used in our experiments was designed analogous to the structure reported in [12,13] albeit with no taper. It was fabricated through the well-established technology of modified chemical vapor deposition (MCVD) technique, which enables a high degree of control on the structural parameters of the preform, and hence the fiber. Use of the MCVD technique also alleviates any issues regarding repeatable fabrication of identical fiber structures, which is sometimes a major concern while fabricating microstructured (holey) fibers. An optical micrograph of the (cleaved) end face of the drawn fiber is shown in Fig. 1 (a) along with the characteristic dimensions. Figure 1 (b) shows the corresponding refractive index profile and the nomenclature. The fabricated fiber had 12 periodic bilayers surrounding the low-index (primarily silica) core. Various dopants as refractive index modifiers of silica were used to realize the synthesized cladding layers and the average refractive indices of the periodic cladding layers were ~1.470 and 1.458. The average thicknesses of the high and low index cladding rings (d_2 and d_1) were measured to be 1.4 μm and 1.6 μm, respectively. The drawn fiber was very robust and could be easily cleaved using a commercial fiber cleaver.

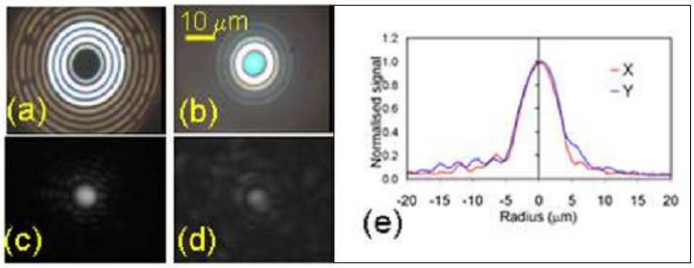

Fig. 2. Near field mode images shown for the white light coupled to (a) cladding and (b) core; (c) core-localized and (d) a higher order mode at 1064 nm; (e) Calibrated fundamental mode profiles in the horizontal x-axis and the vertical y-axis.

A 48 cm section of the fiber was used to measure and record the mode profile of the fiber. As a first step, white light from a tungsten bulb was coupled into a standard silica fiber (SMF) (Corning SMF-28) and butt-coupled with index matching gel to the Bragg fiber. Comparison between Figs. 2(a) and (b) clearly shows that light is tightly confined within the core when the exit end of the illuminated SMF-28 fiber is aligned with the core of the Bragg fiber as opposed to when it is aligned with the cladding rings. Subsequently, light from a CW laser source emitting at 1064 nm was launched into the fiber using a 0.2 NA microscope objective. Figures 2 (c) and (e) show the near field output and transverse intensity profile of the fundamental mode (FM) of the fiber, respectively. The mode field diameter was measured to

#112382 - $15.00 USD Received 4 Jun 2009; revised 4 Sep 2009; accepted 5 Sep 2009; published 11 Sep 2009

be 7.9 μm at 1064 nm. Figure 2(d) shows a higher order mode structure of the fiber with increased throughput light in the cladding layers that could be ascribed to a lossy higher order mode as was observed by deliberately inducing a small misalignment between the test fibre and the SMF-28 fiber. The tungsten source was then used to record the insertion loss spectrum of a 5 cm length of the fiber (Fig. 3(a)). Transmission loss measurements were performed at 1064 nm using the cutback method on the 48 cm long sample of the fiber. The propagation loss was measured to be ~11 dB/m at this wavelength with a coupling loss of ~5.5 dB.

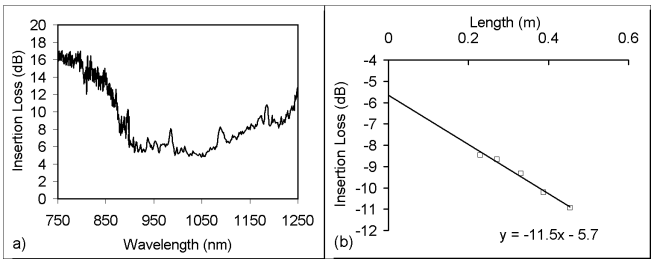

Fig. 3. (a) Insertion loss spectrum of a 5 cm length of the fiber and (b) Results of cutback measurement performed at 1064 nm.

The nonlinear propagation properties of the Bragg fiber were studied by using a frequency doubled idler output from a 1 kHz femtosecond optical parametric amplifier (OPA) system. The OPA was tuned to 1067 nm and the pulses had a FWHM of 120 fs. Three different incident peak powers were used 290 kW, 208 kW and 67 kW. This corresponded to launched peak powers of 82 kW, 59 kW and 19 kW taking into account the launch loss of 5.5 dB. The pulses were launched into different length sections of the Bragg fiber using a (x10) 0.2 NA microscope objective. The output was collected with a 600 μm core diameter silica fiber and the spectrum was recorded using near infrared (Ocean Optics NIR512) and visible (Ocean Optics HR2000) spectrometers. Spectral broadening is evident in the transmitted spectrum shown in Fig. 4(a) with just 3 cm of Bragg fiber. Spectra for the three different launched peak powers are also shown. Five other lengths of the fiber were also examined at these peak powers and the spectra for the 59 kW case for 20 cm, 30 cm, 50 cm, 100 cm and 350 cm are shown in Fig. 4(b). As expected, the peaks near the central wavelength of the input pulse are dominated by self-phase modulation whereas the peak at ~950 nm is due to the influence of dispersive waves whose proximity to the center of the input pulse could be attributed to the relatively large value of the dispersion slope (0.385 ps/(km.nm^2) at 1067 nm) [18].

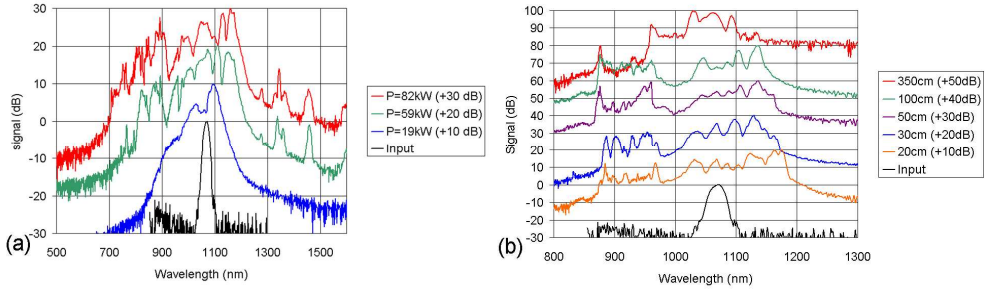

Fig. 4. (a) Spectral broadening in a 3 cm section of Bragg fiber showing (from bottom to top curve) the input pulse spectrum, 19 kW, 59 kW and 82 kW launched peak power and (b) evolution of the spectral broadening for selected lengths of Bragg fiber.

3. Numerical simulation

The experimental results presented above were compared against numerical simulations of linear propagation characteristics and nonlinear pulse evolution in the fiber. The refractive index contrast amongst the various layers in the fabricated Bragg fiber was < 0.6% thereby

#112382 - $15.00 USD Received 4 Jun 2009; revised 4 Sep 2009; accepted 5 Sep 2009; published 11 Sep 2009

making it a weakly guiding structure. Consequently, the LP_{01} mode would constitute the fundamental mode (FM) of the fiber. The dispersion and loss characteristics of the FM were studied by using the Finite Element Method (FEM), which was implemented via the commercial FEM package Comsol Multiphysics. The fiber was assumed to have a core radius of 6 μm and core refractive index of 1.454 at 1060 nm. Figure 5 (a) shows the dispersion and radiation loss spectrum of the modeled fiber. Interestingly the dispersion spectrum has resemblance to that of an air core Bragg fiber [14]. The zero dispersion wavelength of the fiber was calculated at around 1050 nm while the effective area and nonlinearity coefficient [15] of the fiber at the pump wavelength of 1067 nm were ~62 μm^2 and 2.1 $(km.W)^{-1}$ respectively. Clearly the theoretically predicted loss of the fiber at this wavelength is much lower than the experimentally measured value, affirming the loss sensitivity of these fibers to the uniformity of the cladding layers. However, it should be possible to reduce the losses considerably so as to make them comparable to the material loss of silica by further optimization of the fiber design and MCVD process [16,17]. We also theoretically studied the dispersion sensitivity of the fiber to the number of cladding layers, which showed that the ZDW is relatively unaffected by a change in the number of cladding layers. This is somewhat expected because of the tight confinement of the FM within the fiber core (cf. Figure 2(c)).

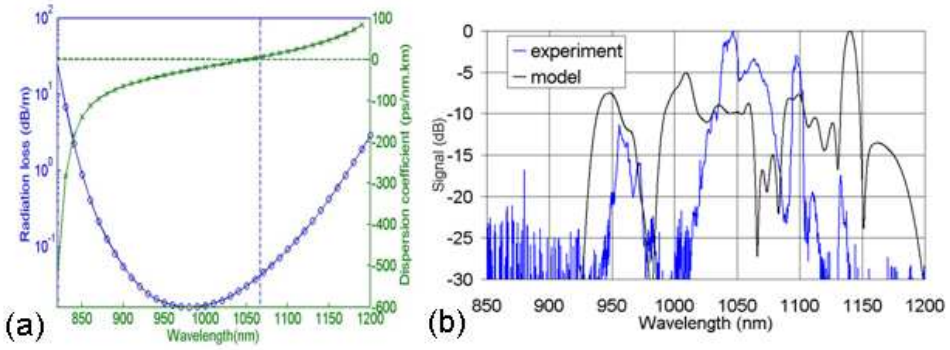

Fig. 5. (a) Simulated dispersion and radiation loss of the Bragg fiber under study and (b) Simulation result (black) and corresponding experimental curve (blue) show spectra in a fiber of length 3.5 m for an input peak power of 59 kW.

Nonlinear pulse propagation was modeled through the generalized nonlinear Schrödinger equation (GNLSE) [15]

$$\frac{\partial A}{\partial z}+\frac{\alpha}{2}A+\beta_1\frac{\partial A}{\partial t}+i\frac{\beta_2}{2}\frac{\partial^2 A}{\partial t^2}-\frac{\beta_3}{6}\frac{\partial^3 A}{\partial t^3}+\ldots= i\gamma\left[1+\frac{i}{\omega_0}\frac{\partial}{\partial t}\right]\left[A(z,t)\int_{-\infty}^{\infty}R(t')\left|A(z,t-t')\right|^2 dt'\right] \quad (1)$$

where $A(z, t)$ is assumed to be the slowly varying amplitude of the propagating mode in a co-moving frame, α is the propagation loss, β_n are different order dispersion terms, γ is the effective nonlinear coefficient of the fiber and $R(t')$ is the Raman response function, which includes both electronic and vibrational Raman contributions. We solved Eq. (1) by employing the symmetrized split-step Fourier scheme with dispersion terms up to sixth order [15]. The input pulse is assumed to be secant hyperbolic in shape with full width at half maximum (FWHM) pulsewidth of 120 fs. We also assumed that the peak power of the pulse was 59kW, which incorporates the power lost due to the coupling loss of 5.5 dB (cf. Figure 3(b)). The width and resolution of the time window and the longitudinal step-size were optimized through a convergence study. Figure 5(b) shows the comparison between experimental and simulated output spectrum of the input pulse centered at 1067 nm at the end of a 3.5 m long Bragg fiber of similar characteristics as the fabricated one. The characteristic

#112382 - $15.00 USD Received 4 Jun 2009; revised 4 Sep 2009; accepted 5 Sep 2009; published 11 Sep 2009

spectral features of the spectrum are in reasonable agreement with the experimentally observed spectrum considering the fabricated fiber parameters and the experimental conditions are not precisely known.

4. Conclusion

Starting from designing and fabricating a solid-core low index contrast silica-based Bragg fiber, we have experimentally characterized it and demonstrated nonlinear spectral broadening in it at a wavelength of ~1 μm. This is the first such demonstration in this class of fiber. The dimensions and mode size of the drawn fiber from this preform were compatible with standard commercial fibers and hence, offer ease of integration with existing devices (such as fiber lasers). The high losses of the fiber may be reduced through a more rigorous control of the preform deposition to reduce bilayer imperfections. In addition, dispersion micromanagement by tapering [19] should allow further optimization of the nonlinear spectral broadening in such specialty fibers. Up-tapering of the fiber (during drawing), which would induce a decrease in dispersion with length, could broaden the spectral bandwidth further [12]. Experimental investigation into this aspect would be the subject of a future publication. The present study shows that solid core silica-based Bragg fibers open up new possibilities in the realm of nonlinear optics as yet another microstructured fiber platform.

Acknowledgements

This work was supported in part by the ongoing Indo-UK collaboration on Microstructured Fibers under the UK-India Education and Research Initiative (UKIERI) project. H. Bookey thanks the Royal Society of Edinburgh for financial support. J. McCarthy acknowledges EPSRC for financial support. S. Dasgupta thanks Dr. F. Poletti for useful discussions on the simulation results.

#112382 - $15.00 USD Received 4 Jun 2009; revised 4 Sep 2009; accepted 5 Sep 2009; published 11 Sep 2009